Magnetic decoupling of Rb spin relaxation in H_2 buffer gas

P. I. Borel,* C. J. Erickson,† and D. K. Walter
Department of Physics, Princeton University, Princeton, New Jersey 08544
(Received 11 June 2002; published 20 December 2002)

We report studies of the magnetic decoupling of Rb spin relaxation in the presence of H_2 buffer gas at high pressures ($\geqslant 1.5$ atm). At low Rb number densities ($\leqslant 5\times10^{13}$ cm^{-3}), we find that the observed magnetic-field dependence of the spin relaxation is almost solely due to binary collisions between Rb atoms and hydrogen molecules, and that it is very well described by three rates: the Rb-Rb spin-exchange rate, the *S*-damping rate, and the Carver rate associated with the hyperfine pressure-shift interaction in collisions of Rb with H_2 molecules. At higher Rb densities, the contribution to the relaxation from Rb triplet dimers becomes significant.

DOI: 10.1103/PhysRevA.66.063410 PACS number(s): 33.35.+r, 31.70.Hq, 32.80.Bx

I. INTRODUCTION

When nuclear spin-polarized noble gases are produced by spin exchange [1] with optically pumped alkali-metal atoms [2], molecular nitrogen is nearly always used to quench the excited alkali-metal atom of the pumping cycle, thereby reducing the large spin-depolarizing effects of radiation trapping. A recent study has shown that despite the chemical reaction of H_2 gas with alkali metals to form alkali hydrides, high nonequilibrium hydrogen densities may persist for several weeks in heated sealed glass cells containing Rb and H_2 [3]. Hence, hydrogen may serve as an alternative quenching gas to nitrogen, especially in applications of hyperpolarized noble gases (such as polarized ^{3}He targets for high-energy scattering experiments) where the dilution of the hyperpolarized nuclei by N_2, with its much higher nuclear charge *Z*, would be profitably avoided.

Hydrogen, like nitrogen and indeed all other inert buffer gases, contributes to the spin relaxation of the optically aligned alkali-metal vapor. In the present work, we investigate experimentally the magnetic-field dependence of the spin relaxation of Rb in the presence of H_2 buffer gas by measuring the relaxation rate ''in the dark,'' utilizing a variation of the method originally introduced by Franzen [4].

II. EXPERIMENTAL SETUP

The single exponential late-time decay rate of the Rb polarization is determined using a previously described experimental arrangement [5,6]. The apparatus is illustrated in Fig. 1. We use spherical glass cells, of diameter $d\approx 2.5$ cm, containing Rb of natural isotopic composition and H_2 gas at several densities from 1.6 to 9 amagat [7]. The cells, inside an oven heated by blowing hot air, are placed in a dc magnetic field *B* (varied from 50 to 6000 G) produced by an electromagnet. The Rb electron spins are polarized by a circularly polarized, resonant D_1 pump beam propagating parallel to the applied magnetic field. The pump light is then blocked with a mechanical chopper and the decay of the electron spin is measured by monitoring the transmitted intensities $I_{\pm}(t)$ of the two helicity components of a weak, linearly polarized probe beam, collinear with the pump, detuned 5–10 Å from the Rb D_2 resonance line. As discussed in Refs. [5] and [6], at late times, the observed decay rate $\gamma_{\rm obs}$ can be found from the signal ratio $V(t)=I_+(t)/I_-(t)$ by use of $\ln\ln[V(t)/V(\infty)]=-\gamma_{\rm obs}t+a$, where $V(\infty)$ is the transmitted signal ratio when the Rb polarization has decayed completely and *a* is an unimportant constant determined by the initial Rb polarization, the Rb number density, the optical path length, and the probe detuning. We verified that the measured rates were independent of the probe-laser power and detuning. Figure 2 shows a typical measurement of a single late-time decay rate.

For a given cell, the late-time relaxation rate $\gamma_{\rm obs}$ was determined as a function of the magnetic field for various temperatures between 125 °C and 225 °C. The H_2 number density $[H_2]$ in each cell was determined by measuring the widths of the pressure-broadened absorption profiles of the Rb D_1 and D_2 lines, as described in Ref. [3]. These measurements were performed both before and after a relaxation measurement in order to monitor possible changes in $[H_2]$ due to hydride formation. We found that $[H_2]$ remained constant for all cells throughout the relaxation rate measurements except in the cell with the highest H_2 density, where the density was observed to drop from 9.2 amagat to 8.8

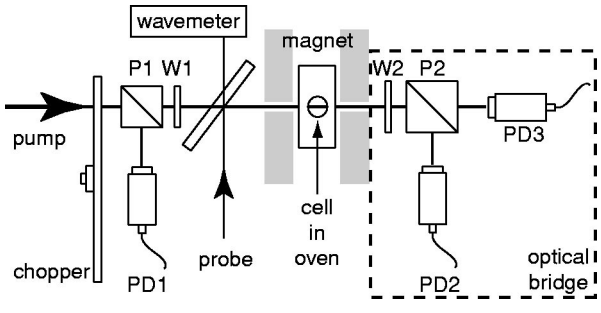

FIG. 1. Experimental setup used to measure the spin decay rate for Rb. The dark interval, caused by the chopper wheel blocking the pump beam, was 20 times the light interval. P1 and P2 denote polarizing beam-splitter cubes, W1 and W2 quarterwave plates, and PD1–PD3 photodiodes.

*Present address: Niels Bohr Institute, Ørsted Laboratory, DK-2100 Copenhagen, Denmark.

†Present address: McKinsey & Co., Chicago, IL 60603.

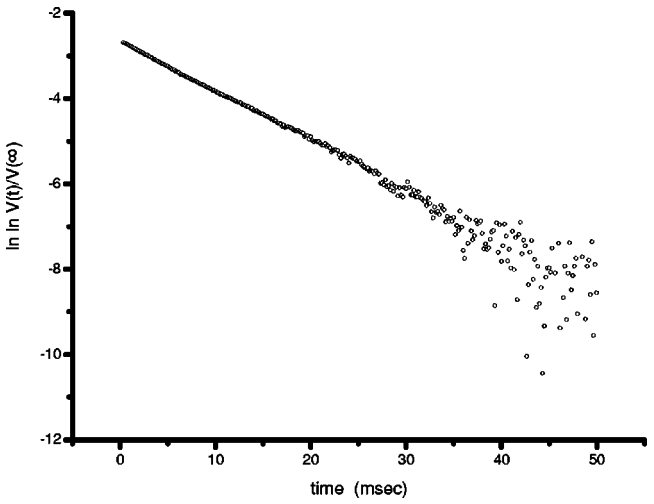

FIG. 2. After sufficiently long time, the decay is characterized by a single exponential time constant $1/\gamma_{\rm obs}$ where $-\gamma_{\rm obs}$ is the slope.

amagat during relaxation measurements at five different temperatures. The Rb number density [Rb] was measured *in situ* by Faraday rotation [8]. Figure 3 shows a representative measurement of the Faraday rotation angle as a function of probe-laser detuning.

Interestingly, we find that the relationship between the Rb number density and the temperature in our cells differs considerably from the Killian formula for saturated vapor pressure [9]. In the low H_2 density cells, the Rb number density was reduced by roughly a factor of 2 compared to the Killian formula, perhaps due to the hydride layer, which rapidly forms at the exposed Rb surfaces. In the high H_2 density cells, the measured Rb number densities were reduced even further. In fact, in the cell with the highest H_2 density, [Rb] appeared to be nearly independent of temperature.

III. DATA ANALYSIS

The main objective of the present study is to investigate the contributions to the Rb spin relaxation from binary collisions between Rb atoms and H_2 molecules. Thus, we correct the observed late-time rate $\gamma_{\rm obs}$ for diffusion to the cell walls and contributions due to Rb triplet dimers in order to obtain the fundamental late-time rate $\gamma^{(1)}$,

$$\gamma^{(1)}=\gamma_{\rm obs}-\gamma_{\rm diff}-\gamma_{\rm trip}. \tag{1}$$

The diffusion correction is given by $\gamma_{\rm diff}=\sqrt{4D\gamma_{\rm obs}/\pi d^2}$, as discussed in Ref. [10]. An additional phenomenon, first discovered by Kadlecek *et al.* [11] and now believed to be due to loosely bound Rb triplet dimers, manifests itself in the magnetic decoupling curves at high Rb number densities. At low buffer-gas densities, the spin-axis interaction in Rb triplet dimers has conclusively been shown to play an important role in the Rb spin relaxation [5]. Kadlecek *et al.* [11] and Erickson [12] have conducted thorough studies on the influence of Rb triplet dimers on the magnetic decoupling curves at high ^{3}He and N_2 buffer-gas densities and have found that this still puzzling effect at a fixed buffer-gas pressure can be characterized by a rate coefficient $k_{\rm trip}$ and magnetic decoupling width ΔB:

$$\gamma_{\rm trip}=\frac{k_{\rm trip}[\mathrm{Rb}]}{1+(B/\Delta B)^2}. \tag{2}$$

We find that all our high-[Rb] data are well parameterized by $\Delta B\sim 1100$ G and $k_{\rm trip}\sim 2.4\times 10^{-14}$ cm^3 s^{-1}, in good agreement with the findings of Ref. [11].

After subtracting these relatively small contributions to the relaxation from diffusion and from Rb triplet dimers, we find that the relaxation rate as a function of the applied magnetic field can be described very well by the model recently presented by Walter *et al.* [6], in which the observed relaxation is the result of three mechanisms: the spin-rotation interaction $\gamma\mathbf{N}\cdot\mathbf{S}$, the hyperfine pressure-shift interaction $\delta A\mathbf{I}\cdot\mathbf{S}$ in binary collisions between Rb atoms and H_2 molecules, and the spin-exchange interaction $J\mathbf{S}_1\cdot\mathbf{S}_2$ in collisions between pairs of Rb atoms. Unlike in Ref. [6], here we use natural Rb rather than pure isotopes, since large amounts of Rb are consumed by hydride formation; as a result, the analysis is slightly more complicated than it is for the single-isotope case.

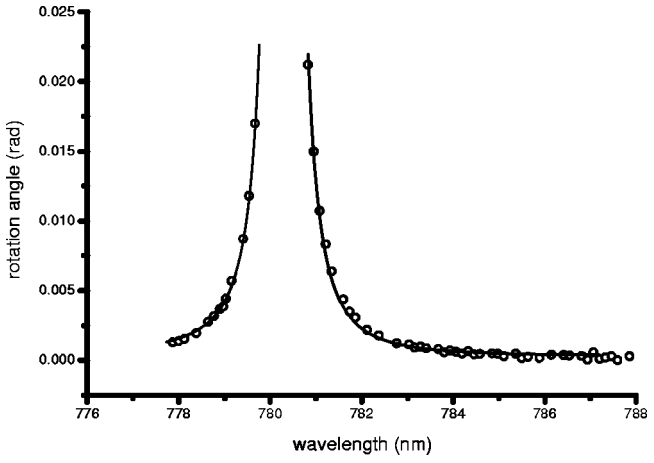

FIG. 3. Faraday rotation angle of the Rb polarization as a function of probe-laser detuning. The Rb number density is extracted as described in Ref. [8].

The spin interactions of a free Rb atom of isotope μ are given by the Breit-Rabi Hamiltonian

$$H_\mu=A_\mu\mathbf{I}_\mu\cdot\mathbf{S}_\mu+g_{\rm S}\mu_{\rm B}BS_{z\mu}, \tag{3}$$

where $\mathbf{I}_\mu$ and $\mathbf{S}_\mu$ are the nuclear and electron spin, respectively, of isotope μ and A_μ is the ground-state hyperfine coupling coefficient. The Schrödinger equation

$$H_\mu|\mu r\rangle=E_{\mu r}|\mu r\rangle \tag{4}$$

defines a set of energies $E_{\mu r}$ and eigenstates $|\mu r\rangle$. The spin polarization of the Rb vapor of mixed isotopes is given by the occupation probabilities ρ_r^μ of sublevel r of isotope μ. Because spin exchange occurs not only between Rb atoms of the same isotope, but also between Rb atoms of different isotopes, the relaxation equation contains terms which couple ρ_r^μ to ρ_s^ν for $\mu\neq\nu$. The full relaxation equation is

$$\frac{d}{dt}\rho_r^\mu = -\sum_{\nu s} \Gamma_{rs}^{\mu\nu}\rho_s^\nu, \tag{5}$$

where the relaxation matrix is

$$-\Gamma_{rs}^{\mu\nu} = \delta_{\mu\nu}[\chi_\mu^2\Gamma_C C_{rs}^\mu + \Gamma_{SD}D_{rs}^\mu] + \Gamma_{EX}E_{rs}^{\mu\nu}. \tag{6}$$

The three characteristic rates associated with the hyperfine pressure-shift interaction, the spin-rotation interaction, and the spin-exchange interaction, respectively, are the Carver rate Γ_C, the *S*-damping rate Γ_{SD}, and the spin-exchange rate Γ_{EX}. The corresponding rate matrices are

$$C_{rs}^\mu = -\delta_{rs}\langle \mu r|(\mathbf{I}_\mu\cdot\mathbf{S}_\mu)^2|\mu r\rangle + |\langle \mu r|\mathbf{I}_\mu\cdot\mathbf{S}_\mu|\mu s\rangle|^2, \tag{7}$$

$$D_{rs}^\mu = -\frac{3}{4}\delta_{rs} + \langle \mu r|\mathbf{S}_\mu|\mu s\rangle\cdot\langle \mu s|\mathbf{S}_\mu|\mu r\rangle, \tag{8}$$

$$E_{rs}^{\mu\nu} = \delta_{\mu\nu}D_{rs}^\mu + \frac{2\eta_\nu}{[I_\mu]}\langle \mu r|S_{z\mu}|\mu r\rangle\langle \nu s|S_{z\nu}|\nu s\rangle. \tag{9}$$

The dimensionless constant χ_μ in Eq. (6), defined as

$$\chi_\mu = \frac{\mu_{1\mu}}{2I_\mu\mu_N}, \tag{10}$$

is the ratio of the hyperfine coupling A_μ of isotope μ (with nuclear spin I_μ and nuclear moment $\mu_{1\mu}$) to the coupling A of a hypothetical Rb isotope with nuclear spin $I=1/2$ and nuclear moment equal to the nuclear magneton μ_N. The χ factors for ^{87}Rb and ^{85}Rb are 0.9170 and 0.2706, respectively. In Eq. (9), $\eta_\nu=[X_\nu]/[X]$ denotes the atom fraction of isotope X_ν of chemical species X, and $[I_\mu]=2I_\mu+1$ is the number of nuclear azimuthal spin states of isotope μ.

The solutions of the relaxation equation (5) are of the form

$$\rho_r^\mu = v_{rk}^\mu e^{-\gamma_k t}, \tag{11}$$

which upon substitution into Eq. (5) yields the eigenvalue equation

$$\sum_{\nu s}(\Gamma_{rs}^{\mu\nu} - \gamma_k\delta_{rs}\delta_{\mu\nu})v_{sk}^\nu = 0. \tag{12}$$

Ordering the non-negative, real decay rates γ_k [13] such that $\gamma_1 \leqslant \gamma_2 \leqslant \cdots \leqslant \gamma_N$, we have

$$\gamma_1 = \gamma_2 = \cdots = \gamma_p = 0, \tag{13}$$

where p is the number of different isotopes. For sufficiently late time t, the polarization decay transients are characterized by the single slowest nonzero rate γ_{p+1}, which is easily extracted from the data. Using Γ_C, Γ_{SD}, and Γ_{EX} as free parameters, we find that the late-time decay rates, corrected for diffusion and triplet dimer contributions, can be fit very well to the foregoing model. In all cases, we find that the best-fit value of Γ_{EX}, within errors on the fit and the measured Rb number density, agrees with previous measurements of the spin-exchange cross section $\sigma_{EX}=\Gamma_{EX}/\bar{v}[\mathrm{Rb}]$ [6,14,15]. Representative measured magnetic decoupling curves for Rb in H_2 are shown in Fig. 4, together with fits to the model.

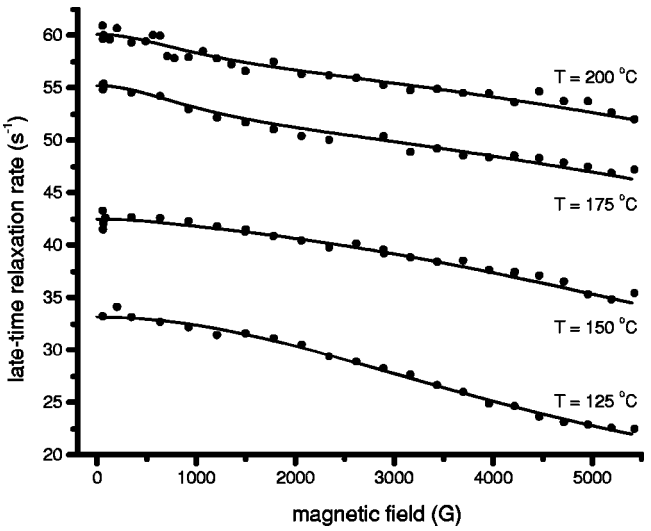

FIG. 4. Measured magnetic decoupling data γ_{obs} (●) and fits $\gamma_{fit}^{(1)}+\gamma_{diff}+\gamma_{trip}$ (—) for Rb in 2.2 amagat H_2.

IV. RESULTS

The measured *S*-damping rates Γ_{SD} due to binary collisions between Rb atoms and H_2 molecules are shown as a function of temperature in Fig. 5. At high Rb number densities, Rb–Rb binary collisions also contribute to the total *S*-damping rate. We take this contribution into account by subtracting $\Gamma_{SD,Rb}=\bar{v}\sigma_{SA}[\mathrm{Rb}]$ from the best-fit values of Γ_{SD}, where $\bar{v}$ is the average relative velocity of the Rb atom pair and σ_{SA} is the binary relaxation cross section, given by $\sigma_{SA}=5.6\times10^{-18}$ cm^2 based on the extensive empirical data in Ref. [12].

We find that Γ_{SD} is well described by

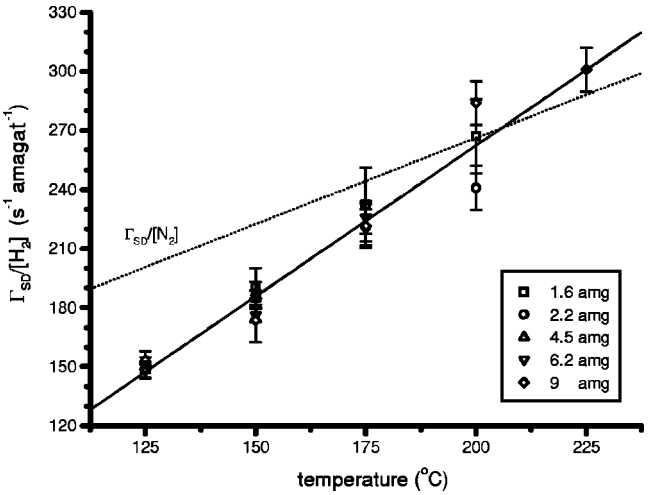

FIG. 5. The measured $\Gamma_{SD}/[H_2]$ as a function of temperature. The solid line is a linear fit to the data. Also shown is $\Gamma_{SD}/[N_2]$ from Ref. [6] (dashed line).

$$\frac{\Gamma_{\mathrm{SD}}}{[\mathrm{H_2}]} = (94 \pm 6)\left(1 + \frac{T - 90\,^{\circ}\mathrm{C}}{(61 \pm 7)\,^{\circ}\mathrm{C}}\right) \quad \mathrm{amagat}^{-1}\,\mathrm{s}^{-1}. \tag{14}$$

For comparison, we note that Ref. [16] reported $\Gamma_{\mathrm{SD}}/[\mathrm{H_2}] = 160$ amagat^{-1} s^{-1} at 35 °C (assuming a slowing-down factor $s = 15.2$) and Ref. [17] found $\Gamma_{\mathrm{SD}}/[\mathrm{H_2}] = 160$ amagat^{-1} s^{-1} at 70 °C (assuming $s = 10.8$).

Comparing our results with those recently obtained by Walter *et al.* [6] for the relaxation of Rb in helium and nitrogen, we find that the *S*-damping rate coefficient at 90 °C of Rb in H_2 is nearly four times larger than that of Rb in ^{3}He, and slightly more than half the *S*-damping rate coefficient of Rb in N_2. Although it may be rather surprising that H_2 causes markedly faster Rb spin relaxation than does helium (which has the same nuclear charge Z), these observations are consistent with the theory of Walker *et al.* [18] for the spin-rotation interaction between alkali-metal atoms and small perturbers such as helium, for which the dominant contribution to the spin-rotation coupling is expected to come from the region external to the core of the perturber (rather than from the region internal to the perturber's core—the case for heavier atoms such as Kr and Xe [19]). In Ref. [18], it is shown that the spin-rotation coupling coefficient γ_a at internuclear separation R of the interaction $\gamma_a \mathbf{N}\cdot\mathbf{S}$ between the alkali-metal electron spin $\mathbf{S}$ and the rotational angular momentum $\mathbf{N}$ of the alkali-metal–He-atom pair is given by

$$\gamma_a(R) = \frac{16\pi^2\hbar^6 a^2 \Delta E_{n_g p}}{3E_p^3 M_{ab} m^2 R^2} |\phi_0(R)|^2 |\phi_{n_g p_z}(R)|^2, \tag{15}$$

where m is the electron mass, M_{ab} is the reduced mass of the atom pair, a is the electron-scattering length from the perturber, $\Delta E_{n_g p}$ is the spin-orbit splitting of the unperturbed first-excited alkali-metal p state (with excitation energy E_p), and ϕ_0 ($\phi_{n_g p_z}$) is the unperturbed wave function of the alkali-metal valence electron in the ground (first-excited p_z) state.

Based on the data for the pressure shift of the alkali-metal absorption lines, the scattering lengths of low-energy electrons from helium and hydrogen are very nearly equal [20,21], and therefore, the difference in the spin-rotation coupling for Rb-He and for Rb-H_2 is due solely to the difference in the reduced mass M_{ab}. Since the cross section is proportional to the collisional average of γ^2, the rate coefficient will scale as $k_{\mathrm{SD}} \sim M^{-5/2}$, including the additional factor of $M^{-1/2}$ from the average relative velocity of the colliding atom pair. Thus for Rb, the *S*-damping rate coefficient in H_2 is expected to be roughly a factor of 3 larger than the *S*-damping rate coefficient in He, in good agreement with the results reported here and in Ref. [6].

At high Rb number densities ($[\mathrm{Rb}] \gtrsim 5 \times 10^{13}$ cm^{-3}), the Carver rate cannot be accurately determined, due to the dominance of the much higher spin-exchange rate, but at lower Rb number densities, we find that a nonzero Carver rate is necessary to obtain satisfactory fits to the theory. From the fits of the theory to the data, we find the Carver rate to be

$$\frac{\Gamma_{\mathrm{C}}}{[\mathrm{H_2}]} = 226 \pm 59 \ \mathrm{amagat}^{-1}\,\mathrm{s}^{-1}. \tag{16}$$

The relatively large error is due to uncertainties in [Rb] and hence in Γ_{EX}. We thus find that the Carver rate for Rb in H_2 has the same magnitude as that for Rb in ^{3}He [6].

ACKNOWLEDGMENTS

The authors thank W. Happer for helpful discussions. The Princeton Atomic Physics group was funded by the AFOSR and NSF; D.K.W. was supported by the Hertz Foundation.

[1] T.G. Walker and W. Happer, Rev. Mod. Phys. **69**, 629 (1997).
[2] W. Happer, Rev. Mod. Phys. **44**, 169 (1972).
[3] P. Borel, W. Griffith, and W. Happer (unpublished).
[4] W. Franzen, Phys. Rev. **115**, 850 (1959).
[5] C.J. Erickson, D. Levron, W. Happer, S. Kadlecek, B. Chann, L.W. Anderson, and T.G. Walker, Phys. Rev. Lett. **85**, 4237 (2000).
[6] D.K. Walter, W.M. Griffith, and W. Happer, Phys. Rev. Lett. **88**, 093004 (2002).
[7] 1 amagat $= 2.687 \times 10^{19}$ cm^{-3}.
[8] Z. Wu, M. Kitano, W. Happer, M. Hou, and J. Daniels, Appl. Opt. **25**, 4483 (1986).
[9] T.J. Killian, Phys. Rev. **27**, 578 (1926).
[10] A.B. Baranga, S. Appelt, M.V. Romalis, C.J. Erickson, A.R. Young, G.D. Cates, and W. Happer, Phys. Rev. Lett. **80**, 2801 (1998).
[11] S. Kadlecek, L.W. Anderson, and T.G. Walker, Phys. Rev. Lett. **80**, 5512 (1998).
[12] C. J. Erickson, Ph.D. thesis, Princeton University, 2000 (unpublished).
[13] Because of the term describing spin exchange between different isotopes, the relaxation matrix $\Gamma_{rs}^{\mu\nu}$ is neither Hermitian nor normal, but all of its eigenvalues are nevertheless real (and non-negative).
[14] H.M. Gibbs and R.J. Hull, Phys. Rev. **153**, 132 (1967).
[15] N.W. Ressler, R.H. Sands, and T.E. Stark, Phys. Rev. **184**, 102 (1969).
[16] R.G. Brewer, J. Chem. Phys. **37**, 2504 (1962).
[17] R.J. McNeal, J. Chem. Phys. **37**, 2726 (1962).
[18] T.G. Walker, J.H. Thywissen, and W. Happer, Phys. Rev. A **56**, 2090 (1997).
[19] Z. Wu, T.G. Walker, and W. Happer, Phys. Rev. Lett. **54**, 1921 (1985).
[20] E. Amaldi and E. Segrè, Nuovo Cimento **11**, 147 (1934).
[21] S. Ch'en and M. Takeo, Rev. Mod. Phys. **29**, 20 (1957).